BioOne COMPLETE

Habitat-specific divergence of air conditioning structures in bird bills

Authors: Danner, Raymond M., Gulson-Castillo, Eric R., James, Helen F., Dzielski, Sarah A., Frank, David C., et al.

RESEARCH ARTICLE

Habitat-specific divergence of air conditioning structures in bird bills

Raymond M. Danner,[1,a]* Eric R. Gulson-Castillo,[2] Helen F. James,[3] Sarah A. Dzielski,[2] David C. Frank III, [2] Eric T. Sibbald,[2] and David W. Winkler[2]

[1] Smithsonian Migratory Bird Center, Smithsonian Conservation Biology Institute, Washington, DC, USA
[2] Department of Ecology and Evolutionary Biology, Cornell University, Ithaca, New York, USA
[3] Department of Vertebrate Zoology, National Museum of Natural History, Smithsonian Institution, Washington, DC, USA
[a] Department of Biology and Marine Biology, University of North Carolina Wilmington, Wilmington, North Carolina, USA
* Corresponding author: dannerr@uncw.edu

ABSTRACT
We used high precision computed tomography (CT) and traditional radiography to study the nasal conchae, complex structures within the nasal cavity that condition air via countercurrent heat exchange. Air conditioning in the conchae assists thermoregulation and water balance, both of which pose challenges for many birds. We hypothesized that hot and water-limited environments would select for larger or more complex conchae to maximize moisture recapture during exhalation and in turn cause the evolution of deeper and wider bills. We provide the first intraspecific comparison of concha size and structure in birds based on CT scans of 15 individuals and radiographs of 39 individuals of 2 subspecies of Song Sparrow (*Melospiza melodia*) that inhabit climatically distinct habitats. CT scans revealed that middle and rostral conchae filled the nasal cavities and had larger surface areas in individuals with larger nasal cavities. The subspecies that inhabits hot and dry coastal dunes (*M. m. atlantica*) had relatively larger conchae and greater overlap of middle and rostral conchae than a nearby inland subspecies that inhabits moister environments (*M. m. melodia*). Radiographs revealed deeper and wider nasal cavities in the dune-endemic subspecies, further indicating they have larger conchae. Locations of maximum complexity of both conchae were more distal in the dune endemic subspecies. These anatomical differences suggest current or past divergent selection pressures on conchae; the larger conchae in the dune subspecies may allow greater water recapture while exhaling. The conchae and external bill are nested structures that were positively related in size and play functionally related roles in thermoregulation, therefore suggesting phenotypic integration. We hypothesize that the typically deeper and wider bill of the dune subspecies has evolved, at least in part, to accommodate larger conchae.

Keywords: nasal conchae, turbinate, thermoregulation, water balance, bill morphology, Song Sparrow, contrast-enhanced CT scan, X-ray

Divergencia dependiente del hábitat en estructuras acondicionadoras del aire de los picos de las aves

RESUMEN
Utilizamos tomografía computarizada (TC) de alta precisión y radiografía tradicional para estudiar los cornetes nasales, los cuales son estructuras complejas dentro de las fosas nasales que acondicionan el aire mediante el intercambio de calor a contracorriente. El acondicionamiento de aire en los cornetes nasales asiste a la termorregulación y al equilibrio hídrico, los cuales presentan retos para muchas aves. Hipotetizamos que ambientes cálidos y limitados de agua favorecerían cornetes más grandes o complejos para maximizar la retención de humedad durante la exhalación y, así, causar la evolución de picos más profundos y anchos. Presentamos la primera comparación intra-específica de tamaños y estructuras de cornetes en aves basándonos en las TC de 15 individuos y las radiografías de 39 individuos de dos subespecies de *Melospiza melodia* que vive en hábitats de climas distintos. Las TC revelaron que los cornetes llenaban las fosas nasales y tenían mayor área superficial en individuos con fosas nasales más grandes. La subespecie que habita en dunas costeras cálidas y secas (*M. m. atlantica*) tenía cornetes medios relativamente más grandes y mayor superposición entre los dos pares de cornetes que la subespecie que habita en ambientes cercanos más húmedos, tierra adentro (*M. m. melodia*). Las radiografías revelaron fosas nasales más profundas y anchas en la subespecie endémica de las dunas, lo cual indica aún más que tienen cornetes más grandes. Las localidades de máxima complejidad en ambos cornetes fueron más distales en la subespecie endémica de las dunas. Estas diferencias anatómicas sugieren que los cornetes experimentan o han experimentado fuerzas de selección divergentes: los cornetes más grandes de la subespecie que habita en dunas quizás permitan la retención de más agua durante la exhalación. Los cornetes y el exterior del pico son estructuras encajadas que estaban positivamente relacionadas en tamaño y tienen funciones relacionadas con la termoregulación, sugiriendo integración fenotípica. Hipotetizamos que los picos típicamente más profundos y anchos de la subespecie de las dunas han evolucionado, por lo menos en parte, para acomodar cornetes más grandes.

Palabras clave: cornetes nasales, conchas nasales, termorregulación, equilibrio hídrico, morfología del pico, *Melospiza melodia*, Tomografía Computerizada TC de alto contraste, rayos X

INTRODUCTION

The environmental factors that give rise to the striking geographic diversity of bird bills have been under study since Darwin (Darwin 1859). Most of this research has focused on external bill morphology and has provided foundational understanding of the processes of evolution, population divergence, and speciation (Lack 1971, Grant 1999). Geographic variation in external bill morphology that results from selection for feeding is supported by correlations with food types (Smith 1990, Remsen 1991, Benkman 1993) and is corroborated by measured selection for feeding over short time periods (Boag and Grant 1981). The bill also functions as a controllable heat dissipater (Hagan and Heath 1980, Tattersall et al. 2009, van den Ven et al. 2016). Geographic relationships between bill size and ambient temperature both among and within several species suggest that bill size and shape are selected directly by climate for their roles in thermoregulation (Snow 1954, Symonds and Tattersall 2010, Greenberg et al. 2011, Greenberg and Danner 2012).

Few studies have focused on the environmental factors that influence evolution of structures that lie within the bill. Likewise, it is unknown if selection on internal and external structures oppose or facilitate one another. Selection on the bill for feeding is thought to extend to the underlying bones and the muscles that power them, as shown by studies of comparative anatomy of closely related species that differ in feeding habits (Bowman 1961, Genbrugge et al. 2011, 2012). Respiratory structures also occupy large spaces within the bill, and they provide the surfaces over which internal and external air make contact during respiration, thus making them important for thermoregulation. Great variation exists among species in respiratory structures within the bill (Bang 1971, King 1993, Yokosuka et al. 2009a), although it is unknown if these structures vary geographically in relation to environmental factors.

Nasal conchae (or turbinates) are complex respiratory structures that lie in the nasal cavities of most birds and mammals and condition air via countercurrent heat exchange (Jackson and Schmidt-Nielsen 1964, Bang and Wenzel 1985, Geist 2000). Nasal conchae also filter air and, in many species, house olfactory nerves and epithelia. For birds, conchae are the primary respiratory structures used for modifying and conditioning respired air during routine ventilation (Geist 2000). During inhalation, conchae are thought to modulate the temperature and humidity of inspired air to more closely resemble the body's internal environment and thus facilitate thermoregulation and water balance (Jackson and Schmidt-Nielsen 1964, Geist 2000). During exhalation, avian nasal conchae recapture moisture and heat from expired air, reducing water and energy loss and warming the surfaces in preparation for
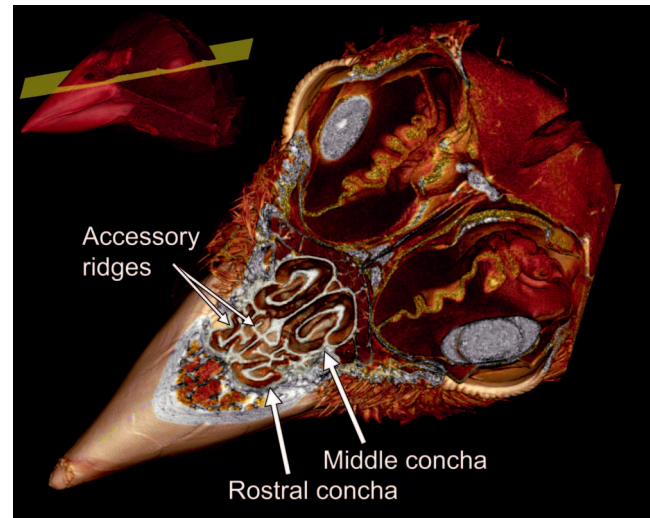

FIGURE 1. Transverse plane of a Song Sparrow head (dorsal view), which reveals the scroll-like middle concha and the complex branching rostral concha with small accessory ridges projecting from the nasal septum and lateral wall of the nasal cavity. Image created from 3D rendering of CT scans. Inset figure shows the external surface of the bird with the location of the plane.

the next inhalation (Tieleman et al. 1999, Geist 2000, Sabat et al. 2006).

Avian nasal conchae typically include 2 or 3 paired, bilaterally symmetrical structures (Figure 1; Video 1 (https://youtu.be/x4ufwDjK2-s); Bang 1971, Ghetie 1976, Bang and Wenzel 1985). Most species have rostral (synonymy: anterior or ventral) and middle (synonymy: maxillary) conchae, and some species also have caudal (synonymy: posterior) conchae (Bang 1971, Ghetie 1976, Bang and Wenzel 1985, King 1993, Yokosuka et al. 2009a, 2009b). A rich vascular plexus lies under the epithelium of the rostral concha in at least some species (Bang and Wenzel 1985). Olfactory epithelium is known to cover the caudal concha and in some taxa the posterodorsal roof of the nasal cavity and at least part of the middle concha (Bang 1971, Bang and Wenzel 1985, Yokosuka et al. 2009a, 2009b). This anatomical arrangement, along with empirical data from Murrish (1973), suggests that the rostral and middle conchae are the primary places of countercurrent heat exchange and air conditioning, and that the caudal concha and the roof of the nasal cavity, as well as the middle concha in some taxa, are the primary sites of olfaction. In some taxa, the conchae are packed tightly into the nasal cavity (Bang 1971, Ghetie 1976), although it is unknown if the external bill is under selection to accommodate the size of the conchae.

Thermoregulation and water balance are intimately linked, and both pose challenges for many birds, which

have high metabolic rates (Gillooly et al. 2001) and maintain high body temperatures. During hot weather, birds can generate substantial excess heat as a result of reduced passive heat loss to the surrounding environment (Speakman and Król 2010). As a result, many species of birds are at risk of hyperthermia if excess heat is not expelled. To avoid hyperthermia, birds dump sizeable amounts of heat through respiratory evaporation at higher ambient temperatures (above a bird's thermoneutral zone; Wolf and Walsberg 1996). Respiratory water loss may cause dehydration in birds, which carry relatively small amounts of extra water, and this threat is exacerbated for species with limited access to fresh water. By contrast, birds must retain heat during cold weather, which is particularly challenging for small birds that experience greater heat loss owing to their high surface area to volume ratios.

We hypothesized that climate directly selects for nasal concha size and structure via the challenges posed by thermoregulation and water balance. We predicted that this selection, related to the local climate, would result in geographic variation in size and structure of the conchae. In the first intraspecific comparison of concha size and structure, we used computed tomography (CT) scans and traditional radiography to characterize and measure the conchae and surrounding anatomy of two closely related subspecies of Song Sparrow (*Melospiza melodia*) that inhabit climatically distinct habitats. *Melospiza m. atlantica* is endemic to the dry sand dunes of the Atlantic coast between North Carolina and New Jersey, USA. *Melospiza m. melodia* is the closely related sister subspecies, which lives across much of the eastern U.S. and inhabits moister environments. Specifically, we predicted that the dune-endemic subspecies would have larger or more complex conchae to provide greater surface area for recapturing moisture when exhaling. Further, we predicted that deeper, wider bills would have larger conchae, thus providing an adaptive explanation for the larger bills that are observed in hotter, dryer places.

METHODS

Terminology
We note that the terms concha and turbinate have been used interchangeably for these structures in birds (e.g., King 1993 vs. Geist 2000). When applied to mammals, turbinate refers to the bony structure, whereas concha refers to the turbinate and tissue covering it. In this paper, we use the term concha to refer to the prominent, bilaterally paired cartilaginous structures that project into the nasal cavities of birds. We describe anatomical planes based on a bird standing in a natural posture and holding its bill roughly parallel with the ground.

Study Taxa and Specimens
To study the nasal conchae with CT scans, we used fluid-preserved specimens, including 8 *M. m. atlantica* (2 females, 6 males) collected on the Delmarva Peninsula, Delaware, and 7 *M. m. melodia* (1 female, 6 males) collected near Washington, DC, during the breeding season (July) of 2013. Following collection, all specimens were frozen in air-tight bags and later fixed in formalin and then transferred to 70% ethanol. Before imaging, specimens were transferred to 100% ethanol for 2 nights to allow adjustment to the new ethanol concentration. They were then soaked in a solution of 1 part iodine to 99 parts of 100% ethanol for 32 or 44 days so that soft tissues and bones could be simultaneously visualized in CT scans. Because specimens shrink when preserved in ethanol and iodine (Vickerton et al. 2013), we took precautions to control for and minimize this shrinkage. First, we incubated specimens in 70% ethanol for >14 days, after which tissue size stabilizes (Vickerton et al. 2013), as recommended by Gignac et al. (2016). Second, we used a minimal concentration of iodine. Third, we did not directly compare specimens preserved in ethanol and iodine to those dried and stuffed. We measured the tarsus (tarsometatarsus) with calipers (precision 0.1 mm) and wing with a wing rule (precision 1 mm). We determined sex by breeding condition and wing length (Pyle 1997).

For additional measurements of nasal cavity dimensions, we radiographed dry stuffed bird skins, consisting of 20 *M. m. atlantica* collected on the Delmarva Peninsula and 19 *M. m. melodia* collected near Washington, DC, all of which are housed at the Smithsonian's National Museum of Natural History. All skins were prepared from birds collected during the breeding season (April–July) between 1876 and 2001 and were identified by the collector as adult males based on signs of breeding condition.

Imaging
Unlike mammals, in which the skeletal structure of the respiratory conchae are typically composed of bone (e.g., Van Valkenbergh et al. 2011), the skeleton of avian conchae is primarily cartilaginous with some regions ossified to varying degrees in different species (Bang 1971). Because cartilage is damaged or destroyed during the preparation of dry museum study skins and skeletons, the gross anatomy of avian conchae has traditionally been studied using histology of fluid-preserved specimens. Contrast-enhanced CT is a relatively new technique that enables simultaneous 3-dimensional (3D) visualization of hard and soft animal tissues (Metscher 2009). We employed this technique to visualize and measure avian conchae in fluid-preserved specimens *in situ*, without sectioning or dissection.

CT scans were performed at the Cornell Imaging Multiscale CT Facility (http://www.ct.cornell.edu). Birds

were removed from the iodine solution the day before scanning, and compressed air was blown through each naris for 10 s to expel ethanol droplets and improve contrast around the conchae. The bill of each bird was covered in tissue and the bird stored in a zip-lock bag until scanned. The birds were scanned in a VersaXRM-520 ZEISS Xradia microscope (Carl Zeiss X-ray Microscopy, Inc., Pleasanton, CA). Scan scale ranged from 16.3 to 20 μm.

We radiographed study skins at the Smithsonian Museum Support Center using a Kevex Microfocus X-ray source (PXS10-16W, Kevex X-Ray Products, Scotts Valley, CA) with a 6-micron focal spot along with a Varian System Flat Panel Amorphous Silicon Digital X-Ray Detector (Pax-Scan 4030R, Varian Medical Systems, Inc., Palo Alto, CA) with a 28.2×40.6 cm pixel area. The product was a 7.1 MB 8 bit TIFF file, captured by Viva k.03 software (Varian Medical Systems, Inc.).

Description of Anatomical Structures and Measurement

To characterize the structure and location of the conchae, nasal cavity, and external morphology, we examined 3D renderings and standardized cross-sections from CT scans and individual radiographs. CT scan measurements were taken using the 3D MPR rendering on OsiriX 5.8.5, 64-bit (Pixmeo SARL). All individual images used were screenshots taken along an axis through each bird's nasal cavity. The axis ran along the nasal septum beginning at the anterior edge of the craniofacial flexion zone and ending at the distal end of the bony nasal cavity (Appendix Figure 5). We took 10 equally spaced frontal (i.e. coronal) cross-sectional screenshots along this axis (Figure 2), starting at the caudal end (i.e. the first section was at the craniofacial flexion zone). The distance between sections averaged 0.570 mm (SE = 0.005 mm, range = 0.517–0.599) and did not differ by subspecies, sex, or structural sizes (tarsus length and wing length; all $t < |1.5|$, all $p > 0.15$).

Using CT scans, we measured complexity differently in middle and rostral conchae. In each frontal cross-section of the middle concha, we counted the number of times the middle concha curled below and above the midpoint and reached the horizontal. For example, if the concha scrolled 1.5 revolutions, we assigned it a score of 3 (Appendix Figure 6). For rostral conchae, we counted how many ridges branched off the main concha body in each section, counting only ridges that were taller than they were wide (Appendix Figure 6).

From CT scans, we measured surface areas of the conchae and external bill as well as linear dimensions of the conchae, nasal capsule, and external bill. We calculated the surface area of the middle and rostral conchae by combining measurements from the 10 frontal cross-sections described earlier and the length of the conchae.

First, on each of the frontal cross-sections, we measured the total linear distance along the edge of the concha that would contact respired air using ImageJ 1.48 (Rasband 2014) and a scale bar from the OsiriX measurement tool. We then sequentially averaged the measurements of adjacent screenshots and multiplied those averages by the distance between each pair of screenshots. Last, we summed those products separately for middle and rostral conchae to estimate surface area for each concha. We measured the length of the concha from the rostral to the caudal tips of each (Appendix Figure 7A and B). To quantify their overlap, we measured the distance between the distal end of the middle concha and the proximal end of the rostral concha parallel to the axis that ran from the ectethmoidal notch to the tip of the nasal cavity (Appendix Figure 7C). To measure nasal cavity size, we took width and depth measurements perpendicular to this axis, where the lateral nasal skeletal bars were visible on those planes and thus provided a consistent landmark (Appendix Figure 7D and E). External bill dimensions, including culmen length, bill width, and bill depth, were taken level with the anterior end of the nares. Total bill length was measured from the bill tip to the craniofacial flexion zone (i.e. frontonasal hinge).

From individual radiographs of dry study skins, we took linear measurements using ImageJ 1.48 (Rasband 2014), including nasal cavity depth from the highest point of the dorsal wall of the nasal cavity to the ventral wall of the nasal cavity (Appendix Figure 8) and width along the ventral wall of the nasal cavity, between the left and right maxillary processes of the nasal bone. We were unable to identify a clear landmark at the base of the bill that would allow measurements of nasal cavity length. From these dry specimens, we also measured external bill length (nalospi), width, and depth at the anterior edge of the nares using calipers (0.01 mm precision).

Analyses

Because we took CT scans and individual radiographs from different groups of specimens, we analyzed those datasets separately. Using measurements from CT scans, we tested for relationships between conchae size and nasal cavity size and between the nasal cavity and external bill morphology. Between subspecies, we compared the surface area and overlap of conchae. We corrected surface area of the conchae by dividing by nasal cavity length because the surface area was correlated with the cavity length (see results). We compared the complexity of the middle and rostral conchae and the position of the maximum complexity of both conchae, which were uncorrected for nasal cavity length. With data from radiographs, we compared nasal cavity size as a proxy for concha size.

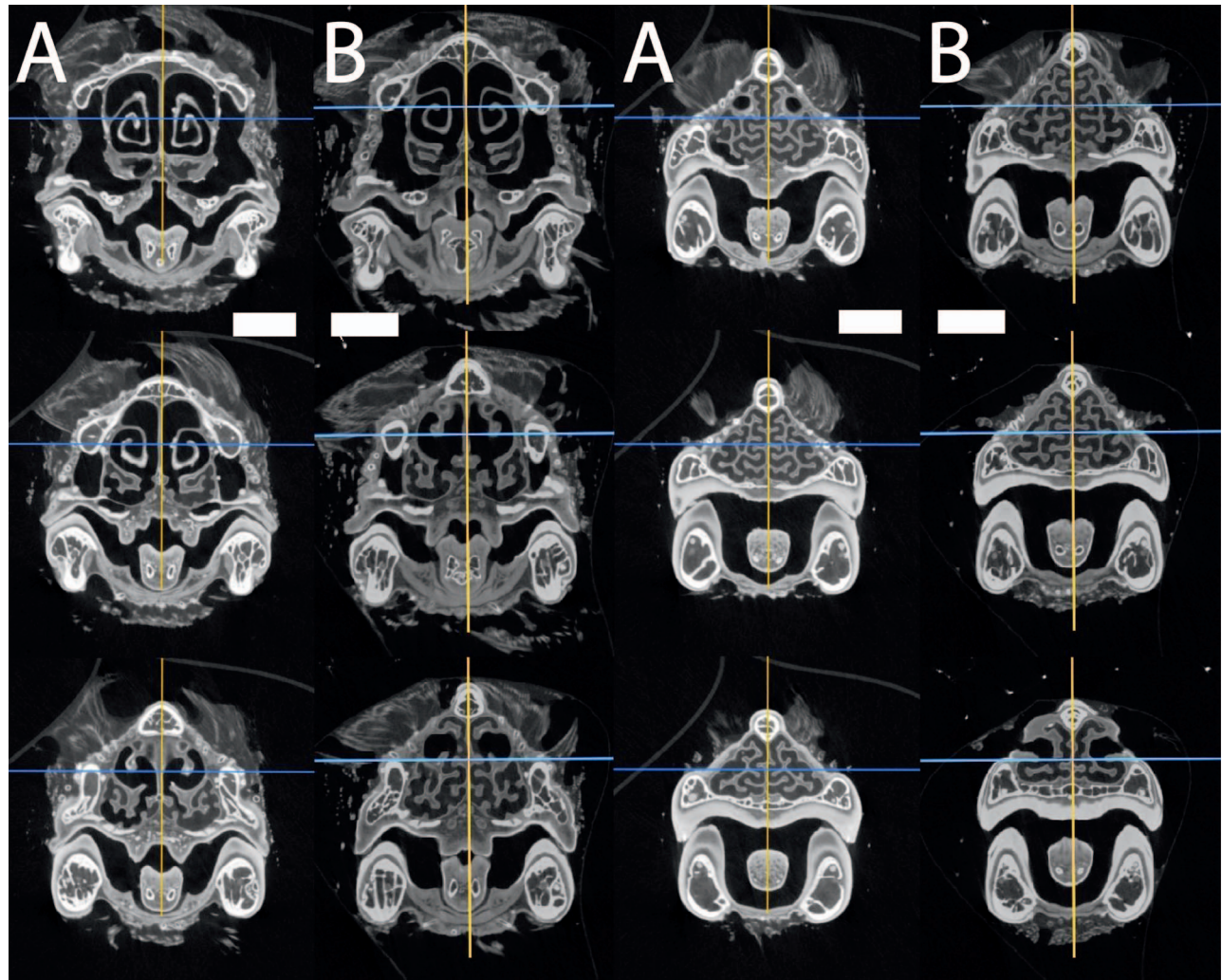We performed all statistics in R (R Core Team 2015). We used linear models (function lm) with a normal error

FIGURE 2. Frontal cross-sections 3–8 of the bill in 2 Song Sparrows, illustrating the differences between (**A**) *M. m. atlantica* and (**B**) *M. m. melodia*. Sections are ordered sequentially, from caudal-most (top left, section 3) to rostral-most (bottom right, section 8). Within each cross-section, the top is dorsal and the bottom is ventral. Note that the complexity has shifted rostral in panel (**A**). Cross-sections are derived from high-resolution CT scans of fluid-preserved specimens. The 4 upper left images show the scroll-like middle conchae, and the right and lower left images show the branched rostral conchae with their accessory ridges. Scale bar = 2.0 mm.

distribution for all comparisons of continuous variables. We visually inspected plots of residuals from linear models and found they were normally distributed. For count data (i.e. complexity of conchae), we used the nonparametric Mann-Whitney U test (function wilcox.test). For comparisons of subspecies we present group means ($\bar{x}_{atlantica}$ and $\bar{x}_{melodia}$), and for relationships between structures we present effect sizes (i.e. B). We also present the associated standard errors for differences, test statistics (t- or z-values), and p-values. We rejected null hypotheses with a p-value <0.05. Because we performed multiple tests of each hypothesis, which increases the probability of a type I error (falsely rejecting the null hypothesis of no difference between subspecies), we adjusted our p-values with the Holm-Bonferroni

correction for each family of hypotheses (Holm 1979) using R function p.adjust.

Subspecies did not differ in structural size (wing length and tarsus length) in either the fluid-preserved or dry specimens (all $t < |0.8|$, all $p > 0.16$), consistent with previous studies of these populations (Greenberg et al. 2012, Danner and Greenberg 2015). Among the fluid-preserved specimens used for CT scans, no differences were found between subspecies in external bill dimensions (all $t < |1.5|$, all $p > 0.17$), suggesting that the sample sizes were too small to detect the differences recorded in other studies (Greenberg et al. 2012, Danner and Greenberg 2015), and also that allometry would not bias intergroup comparisons of other morphological features. Among the larger sample of study skin specimens that we radio-
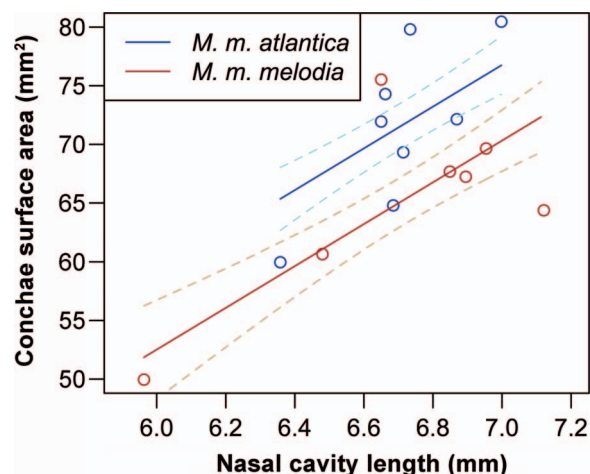
FIGURE 3. Conchae surface area in relation to nasal cavity length in 2 subspecies of Song Sparrow. Points = raw data, solid lines = model predictions, dashed lines = predicted standard error.

graphed, the dune endemic subspecies had wider, deeper, and longer bills at the nares, and as a result had greater bill surface areas (all $t > |2.7|$, all $p < 0.009$), consistent with previous studies (Greenberg et al. 2012, Danner and Greenberg 2015). Nasal cavity size was not related to the date the specimen was collected (both $t < |1.2|$, $p > 0.25$), indicating that collection date did not bias intergroup comparisons.

RESULTS

Description of Anatomical Structures

As shown in the CT images (Figure 1), 2 conchae dominate the interior space of the nasal cavity in the Song Sparrow and effectively divide the cavity into 2 connected chambers. Air inspired through the naris first enters the nasal vestibule and encounters the rostral concha, a complex structure consisting of a central plate suspended from the dorsolateral wall of the nasal cavity, with a number of ridges projecting from it at approximately right angles (usually 5 ridges in our sample). In cross-section, this concha appears as a branching structure (Figure 1 and 2). The ridges of the rostral concha interdigitate with smaller ridges that arise from the nasal septum and the lateral wall of the nasal vestibule (usually 3 from the nasal septum and 2 from the lateral wall; Figure 2). Air next enters the space dominated by the middle concha, a simpler scroll-shaped structure with an arched roof dorsally, suspended again from the dorsolateral wall of the nasal cavity. The middle concha is coiled to varying degrees but usually ~1.5 times at the maximum. After flowing over the middle concha, inspired air can progress through the pharynx and down the trachea.

The rostral concha and its accessory ridges occupy the space from the front of the nasal cavity to slightly posterior to the external naris. Toward its posterior terminus, it is overlain dorsally by the middle concha with its surrounding space or chamber. That chamber extends from just posterior to the external naris back beyond the bill into the antorbital space, posteriorly. The chamber defined by the middle concha extends all the way to the ectethmoid plate. We did not observe a third caudal concha in the CT scans of Song Sparrow heads.

The middle and rostral conchae, together with interdigitating ridges, fill the nasal cavity along both left–right and dorsoventral axes; their size is restricted by the surrounding dimensions of the bony maxilla and to a lesser extent the antorbital space (example in Figure 1). Based on measurements from CT scans, external bill depth was related to nasal cavity depth at the lateral nasal bars ($B = 2.25$ mm $\pm$ 0.60 SE, $t_{13} = 3.8$, $p = 0.002$, $r^2 = 0.52$), and external bill width tended to be related to nasal cavity width ($B = 1.07$ mm $\pm$ 0.52 SE, $t_{13} = 2.1$, $p = 0.06$, $r^2 = 0.25$). Along the anteroposterior axis, longer nasal cavities housed longer middle and rostral conchae (middle: $B = 0.76$ mm $\pm$ 0.17 SE, $t_{13} = 4.5$, $p < 0.002$, $r^2 = 0.61$; rostral: $B = 0.42$ mm $\pm$ 0.19 SE, $t_{13} = 2.2$, $p < 0.05$, $r^2 = 0.27$). Longer nasal cavities housed conchae with larger surface areas (middle: $B = 8.22$ mm^2 $\pm$ 3.77 SE, $t_{13} = 2.2$, $p = 0.048$, $r^2 = 0.27$; rostral: $B = 9.73$ mm^2 $\pm$ 3.33 SE, $t_{13} = 2.9$, $p = 0.024$, $r^2 = 0.35$). External bill surface area correlated with surface area of conchae ($B = 0.36$ mm^2 $\pm$ 0.14 SE, $t_{13} = 2.7$, $p = 0.021$, $r^2 = 0.39$).

Subspecies Comparisons

Based on CT scans, after correcting for nasal cavity length, surface area of conchae was significantly larger in the dune endemic subspecies ($\bar{x}_{atlantica} = 71.6$ mm^2 $\pm$ 2.64 SE, $\bar{x}_{melodia} = 64.7$ mm^2 $\pm$ 3.25 SE, $t_{13} = -2.33$, $p < 0.01$; Figure 3). Independent measurements of the middle and rostral conchae (corrected for nasal cavity length) tended to be larger in the dune endemic subspecies (middle: $\bar{x}_{atlantica} = 32.5$ mm^2 $\pm$ 1.39 SE, $\bar{x}_{melodia} = 28.9$ mm $\pm$ 1.98 SE, $t_{13} = -1.84$, $p = 0.09$; rostral: $\bar{x}_{atlantica} = 39.0$ mm^2 $\pm$ 1.52 SE, $\bar{x}_{melodia} = 35.8$ mm $\pm$ 1.81 SE, $t_{13} = -1.89$, $p = 0.08$). The middle concha of the dune endemic extended farther anterior than in the interior subspecies (Figure 4 vertical lines; $\bar{x}_{atlantica} = 5$ sections $\pm$ 0 SE sections and $\bar{x}_{melodia} = 4.3$ sections $\pm$ 0.2 SE), creating greater overlap with the rostral concha ($\bar{x}_{atlantica} = 2.5$ mm $\pm$ 0.20 SE, $\bar{x}_{melodia} = 1.57$ mm $\pm$ 0.32 SE, $t_{13} = -2.30$, $p < 0.04$). The location of maximum complexity tended to be shifted anterior in the dune endemic subspecies in both the middle concha ($\bar{x}_{atlantica} = 3.5$ sections $\pm$ 0.10 SE, $\bar{x}_{melodia} = 3.21$ sections $\pm$ 0.11 SE, $t_{13} = -2.1$, $p = 0.06$) and the rostral concha ($\bar{x}_{atlantica} = 7.75$ sections $\pm$ 0.17 SE, $\bar{x}_{melodia} = 7.21$ sections $\pm$ 0.11 SE, $t_{13} = -2.7$, $p = 0.04$). The
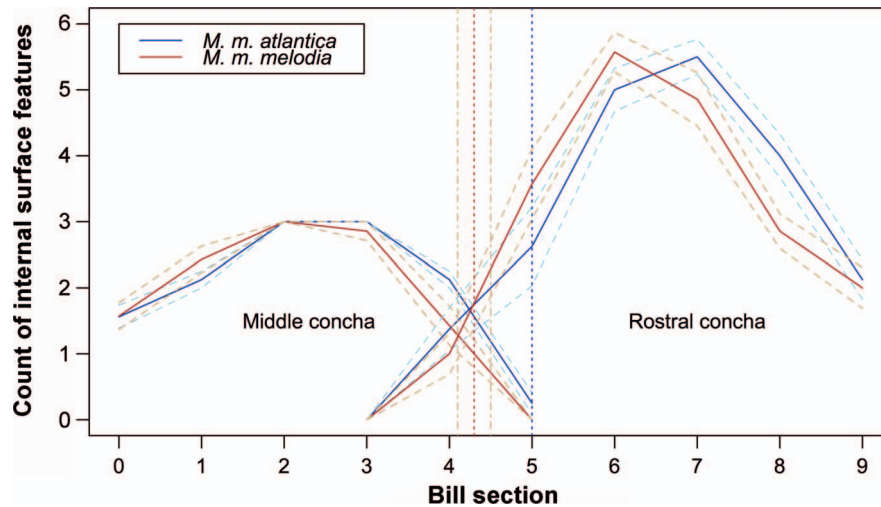
FIGURE 4. Count of concha complexity across 10 cross-sections of 2 subspecies of Song Sparrow. Solid lines = mean, dashed lines = standard error. The x-axis is the number of the frontal cross-section of the bill, from caudal to rostral, where 0 = the craniofacial flexion zone and 9 = the distal end of the nasal cavity. Vertical dotted lines indicate the mean of the rostral terminus of the middle concha. In *M. m. atlantica*, the rostral terminus was always at section 5, hence the lack of error bars.

maximum complexity did not differ between subspecies; all individuals had a maximum of 3 internal surface features in each middle conchae, and rostral conchae had a range of 4–6 features ($\bar{x}_{atlantica} = 5.87 \pm 0.13$ SE, $\bar{x}_{melodia} = 5.57 \pm 0.32$ SE, $W = 33$, $p = 0.46$).

Among study skins, radiographs showed that the dune endemic subspecies had nasal cavities that were both deeper ($\bar{x}_{atlantica} = 2.52$ mm ± 0.038 SE, $\bar{x}_{melodia} = 2.40$ mm ± 0.022 SE, $t_{40} = -3.5$, $p = 0.001$; controlled for tarsus length by including tarsus length as an additive variable) and wider ($\bar{x}_{atlantica} = 4.08$ mm ± 0.030 SE, $\bar{x}_{melodia} = 3.93$ mm ± 0.017 SE, $t_{40} = -4.3$, $p < 0.001$) than those of the inland subspecies.

DISCUSSION

Description of Anatomical Structures
In the Song Sparrow, the conchae together with accessory ridges fill the nasal cavity and provide surface area to condition inspired air before it enters the lungs and to recapture moisture from expired air. The conchae of the Song Sparrow exhibit both differences and similarities with conchae of other species. The structure of the nasal conchae has previously been documented in only 15 passerine families and 26 species, to our knowledge, none of which were found to have an elaborate rostral concha with interdigitating accessory ridges as found in *M. melodia* (Bang 1971, Yokosuka et al. 2009a, 2009b). In nearly all other birds studied, the nasal septum is free of even minor projections. The tube-nosed seabirds (Procellariiformes) are exceptions to the rule; they are the only birds in which a concha has been previously reported to arise from the nasal septum (Bang 1965). This concha is olfactory in function (Bang 1965),

however, and is not associated with the rostral respiratory conchae, which are themselves greatly reduced or occluded, putatively to protect internal structures while plunge-diving (Geist 2000). Whether the elaborate respiratory structures densely filling the nasal vestibule we observed in the Song Sparrow are typical of new world sparrows is unknown.

The structure of the middle concha and lack of a caudal concha are similar to descriptions of other taxa (Bang 1971, Yokosuka et al. 2009a, 2009b). The middle conchae occupy the greater part of the bill posterior to the nares as well as much of the antorbital space, and they comprise the majority of the soft structure inside the nasal cavities. The middle concha has the typical scroll-like form found in most other birds (Bang 1971). The apparent absence of a distinct caudal olfactory concha in the Song Sparrow is consistent with reports of other passerines in which the caudal concha is described as either a mound or lacking entirely (Bang 1971, Yokosuka et al. 2009a, 2009b). The poorly developed or absent olfactory concha by itself tells us little about the olfactory abilities of the Song Sparrow. In the passerine birds examined by Bang (1971), olfactory epithelium was frequently present on the caudodorsal roof of the nasal cavity and sometimes on the nasal septum.

Subspecies Comparisons
The anatomical differences between the dune endemic *M. m. atlantica* and sister subspecies *M. m. melodia* suggest current or past divergent selection pressures on nasal conchae. First, the larger surface area of the conchae in the dune endemic subspecies would seem to allow greater water condensation during exhalation, thus presumably facilitating improved water efficiency. Geist (2000) found

that functional conchae resulted in savings of 55–71% of respiratory water loss in 4 species of temperate-zone birds. The large potential water savings afforded by conchae suggests that increases or decreases in surface area may lead to significant changes in water conservation. Second, we found that the locations of maximum complexity within the conchae were more distal in the dune endemic subspecies. The functional significance of this shift is unknown. Tieleman et al. (1999) hypothesized that longer bills may allow greater cooling capacity and therefore greater potential for water recapture. A potential mechanism underlying this relationship is that longer bills position condensing surfaces distally, farther from the core of the bird, thus providing cooler surfaces, which may facilitate condensation of expired air.

To our knowledge, the structure of avian conchae has not previously been compared across a moisture gradient. Geist (2000) noted in a personal observation that 4 species within 1 family (Phasianidae) that inhabit different climate zones appear qualitatively similar, although measurements are not provided. Tieleman et al. (1999) and Sabat et al. (2006) hypothesized that species of larks (*Ammomanes deserti* and *Galerida cristata*) and populations of Rufous-collared Sparrow (*Zonotrichia capensis*), respectively, would have larger or more complex conchae in arid locations, which would result in greater water efficiency. They found that the taxa from arid habitats did not recover more moisture in the nasal passages, although they did not test whether the structure of the conchae varied along the moisture gradient. Similarly, Schmidt-Nielson et al. (1970) found no difference in exhaled air temperature (a proxy for water recapture in the nasal cavity) among 7 species of birds (many from different families) that inhabit deserts vs. more moderate environments, although the structures of conchae were not measured. To understand the functional anatomy of conchae, comparisons of evaporative water loss, breathing rates, and simulated airflow should focus on taxa with described differences in concha structure, such as our study populations.

Among mammals, interspecific divergence in conchae and the bony turbinates has been shown along the transition from land to salt water, suggesting adaptation to those environments. Van Valkenburgh et al. (2011) showed that aquatic and semiterrestrial mammals of saltwater environments tend to have relatively larger respiratory conchae than their terrestrial relatives. Van Valkenburgh et al. (2011) hypothesized that larger respiratory conchae have evolved to increase water and heat retention in response to the limited fresh water in marine environments and greater potential for heat loss underwater. The large respiratory conchae of elephant seals (*Mirounga angustirostris*) contribute to this species' ability to retain up to 92.5% of the water contained in each breath (Lester and Costa 2006).

Although larger conchae putatively improve water conservation, they may also recapture more body heat, potentially posing a challenge for animals that inhabit hot climates, such as the dune-endemic *M. m. atlantica*; however, the potential of respiratory conchae to conserve heat seems to be greatest at lower ambient temperatures. Geist (2000) estimated that at a cool temperature (15 °C), the conchae of 4 temperate zone bird species conserve 3.5–6.1% of the daily energy budget. Schmidt-Nielsen et al. (1970) and Murrish (1973) used physical and physiological principles to estimate that heat recapture declines at higher temperatures, when heat loss would be advantageous, suggesting that larger conchae would not be a liability in hot conditions.

The conchae and external bill of the Song Sparrow are tightly nested structures, positively correlated in size, and have related functions of heat and water balance (Greenberg et al. 2012, Danner and Greenberg 2015), suggesting they are phenotypically integrated (Pigliucci 2003) and evolve in tandem. We hypothesize that in our system, the larger external bill of the dune population has evolved, at least in part, to accommodate larger conchae. Because the dune birds experience hot, dry summer conditions but relatively mild winters (Danner et al. 2016), we expect the season of critical thermal stress to be summer (Danner and Greenberg 2015). As a result, we expect selection to favor both larger conchae and external bill surface area in the dune-endemic subspecies. Regarding the interior population, Danner and Greenberg (2015) hypothesized that winter is the season of critical thermal stress because winters are cold, and, although summers are hot, moisture is plentiful. In interior populations, we therefore expect selection for smaller bill surface area in the winter to minimize heat loss. Larger conchae would theoretically improve heat recapture in interior winters, however, thus raising the possibility that the smaller bills constrain the size of conchae in that population and that the season of critical thermal stress may differ from organ to organ (i.e. external bill vs. conchae).

Although we generally hypothesize that the hot/dry and cool/moist climates in our system select for positively correlated sizes between concha and external bill size, other climates may select different relative sizes of these structures. For example, in cold and dry systems we might expect birds to minimize bill surface area to reduce heat loss yet maximize concha size and complexity to recapture water and heat. In hot and moist environments, however, we expect small conchae because there is a lower premium on water, yet larger bill surface area for heat dissipation because heat loss through evaporative water loss is less effective in humid environments. In climates with ambient temperatures that frequently rise above the body temperature of the organism, we expect smaller bills to reduce heat gain from the environment (Greenberg and Danner 2012). Further, because the respiratory conchae are expected to heat up to body temperature or above, they would not function as counter-

current heat exchangers at temperatures above body temperature and would therefore not recapture moisture; the type of selection on conchae, or lack thereof, is unclear in this situation. Last, adaptation of conchae to specific climates may include the evolution of complexity independent of size. Note that many variables likely influence the evolution of concha size and external bill morphology, and thus these patterns may not be found in all taxa.

Our study reveals that respiratory conchae of the Song Sparrow are more complex in structure than expected and provides the first evidence that conchae can vary in size and structure within a species, between habitats. Contrast-enhanced CT scanning enables the morphology of these cryptic structures to be conveniently visualized and compared, which should facilitate further study of avian conchae in ecological and evolutionary contexts. To better understand function of concha structure and size, researchers could pair anatomical information with measured or expected abilities of air conditioning under various climatic conditions. In addition, our results with the Song Sparrow illustrate that much work remains to be done to simply characterize nasal conchae among avian taxa, particularly among passerines.

ACKNOWLEDGMENTS

LITERATURE CITED

Bang, B. G. (1965). Anatomical adaptations for olfaction in the snow petrel. Nature 205:513–515.

Bang, B. G. (1971). Functional anatomy of the olfactory system in 23 orders of birds. Acta Anatomica Supplementum 58:1–76.

Bang, B., and B. Wenzel (1985). Nasal cavity and olfactory system. Form and function in birds 3:195–225.

Benkman, C. W. (1993). Adaptation to single resources and the evolution of crossbill (*Loxia*) diversity. Ecological Monographs 63:305–325.

Boag, P. T., and P. R. Grant (1981). Intense natural selection in a population of Darwin's Finches (Geospizinae) in the Galapagos. Science 214:82–85.

Bowman, R. I. (1961). Morphological differentiation and adaptation in the Galápagos finches. University of California Press, Berkeley and Los Angeles, CA.

Danner, R. M., and R. Greenberg (2015). A critical season approach to Allen's Rule: Bill size declines with winter temperature in a cold temperate environment. Journal of Biogeography 42:114–120.

Danner, R. M., B. J. Olsen, and D. L. Luther (2016). Migratory status, winter subspecies interactions, and habitat segregation of Atlantic Song Sparrows (*Melospiza melodia atlantica*). The Wilson Journal of Ornithology 128:434–437.

Darwin, C. (1859). The Origin of Species by Means of Natural Selection, or The Preservation of Favored Races in the Struggle for Life, first edition. John Murray, London, United Kingdom.

Geist, N. R. (2000). Nasal respiratory turbinate function in birds. Physiological and Biochemical Zoology 73:581–589.

Genbrugge, A., D. Adriaens, B. De Kegel, L. Brabant, L. Van Hoorebeke, J. Podos, J. Dirckx, P. Aerts, and A. Herrel (2012). Structural tissue organization in the beak of Java and Darwin's finches. Journal of Anatomy 221:383–393.

Genbrugge, A., A. Herrel, M. Boone, L. Van Hoorebeke, J. Podos, J. Dirckx, P. Aerts, and A. Dominique (2011). The head of the finch: The anatomy of the feeding system in two species of finches (*Geospiza fortis* and *Padda oryzivora*). Journal of Anatomy 219:676–695.

Ghetie, V. (1976). Anatomical Atlas of Domestic Birds. Academiei Republicii Socialiste Romania. 294 pp.

Gignac, P. M., N. J. Kley, J. A. Clarke, M. W. Colbert, A. C. Morhardt, D. Cerio, I. N. Cost, P. G. Cox, J. D. Daza, C. M. Early, and M. S. Echols (2016). Diffusible iodine-based contrast-enhanced computed tomography (diceCT): An emerging tool for rapid, high-resolution, 3-D imaging of metazoan soft tissues. Journal of Anatomy 228:889–909.

Gillooly, J. F, J. H. Brown, G. B. West, V. M. Savage, and E. L. Charnov (2001). Effects of size and temperature on metabolic rate. Science 21:2248–2251.

Grant, P. R. (1999). Ecology and Evolution of Darwin's Finches. Princeton University Press Princeton, NJ, USA.

Greenberg, R., V. Cadena, R. M. Danner, and G. Tattersall (2012). Heat loss may explain bill size differences between birds occupying different habitats. PLOS One **7**:e40933. doi:10.1371/journal.pone.0040933

Greenberg, R., R. Danner, B. Olsen, and D. Luther (2011). High summer temperature explains bill size variation in salt marsh sparrows. Ecography 35:146–152.

Greenberg, R., and R. M. Danner (2012). The influence of the California marine layer on bill size in a generalist songbird. Evolution 66:3825–3835.

Hagan, A. A., and J. E. Heath (1980). Regulation of heat loss in the duck by vasomotion in the bill. Journal of Thermal Biology 5: 95–101.

Hillenius, W. J. (1992). The evolution of nasal turbinates and mammalian endothermy. Paleobiology 18:17–29.

Holm, S. (1979). A simple sequentially rejective multiple test procedure. Scandinavian Journal of Statistics 6:65–70.

Jackson, D. C., and K. Schmidt-Nielsen (1964). Countercurrent heat exchange in the respiratory passages. Proceedings of the National Academy of Sciences USA 51:1192–1197.

King, A. (1993). Apparatus respiratorius (systema respiratorium). In Handbook of Avian Anatomy: Nomina Anatomica Avium, second edition (J. J. Baumel, Ed.). Publications of the Nuttall Ornithological Club 23:257–299.

Kingsolver, J. G., and T. L. Daniel (1983). Mechanical determinants of nectar feeding strategy in hummingbirds: Energetics, tongue morphology, and licking behavior. Oecologia 60:214–226.

Lack, D. (1971). Ecological isolation in birds. Harvard University Press, Cambridge, MA, USA.

Lester, C. W., and D. P. Costa (2006). Water conservation and fasting in northern elephant seals (*Mirounga angustirostris*). Journal of Experimental Biology 209:4283–4294.

Metscher, B. D. (2009). MicroCT for developmental biology: A versatile tool for high-contrast 3D imaging at histological resolutions. Developmental Dynamics 238:632–640.

Murrish, D. E. (1973). Respiratory heat and water exchange in penguins. Respiration Physiology 19:262–270.

Pigliucci, M. (2003). Phenotypic integration: Studying the ecology and evolution of complex phenotypes. Ecology Letters 6:265–272.

Pyle, P. (1997). Identification Guide to North American Birds, Part I: Columbidae to Ploceidae. Slate Creek Press, Bolinas, CA, USA.

R Core Team (2015). R: A language and environment for statistical computing. R Foundation for Statistical Computing, Vienna, Austria. http://www.R-project.org/

Rasband, W.S. (2014). ImageJ, U.S. National Institutes of Health, Bethesda, Maryland, USA. http://imagej.nih.gov/ij/

Remsen, J. V. (1991). The community ecology of Neotropical kingfishers. University of California Publications in Zoology 124:1–116.

Sabat, P., G. Cavieres, C. Veloso, and M. Canals (2006). Water and energy economy of an omnivorous bird: Population differences in the Rufous-collared Sparrow (*Zonotrichia capensis*). Comparative Biochemistry and Physiology Part A: Molecular & Integrative Physiology 144:485–490.

Schmidt-Nielsen, K., F. R. Hainsworth, and D. E. Murrish (1970). Counter-current heat exchange in the respiratory passages: Effect on water and heat balance. Respiration Physiology 9: 263–276.

Smith, T. B. (1990). Resource use by bill morphs of an African finch: Evidence for intraspecific competition. Ecology 71:1246–1257.

Snow, D. (1954). Trends in geographical variation in palaerctic members of the genus *Parus*. Evolution 8:19–28.

Speakman, J. R., and E. Król (2010). Maximal heat dissipation capacity and hyperthermia risk: Neglected key factors in the ecology of endotherms. Journal of Animal Ecology 79: 726–746.

Symonds, M. R. E., and G. J. Tattersall (2010). Geographical variation in bill size across bird species provides evidence for Allen's rule. The American Naturalist 176:188–197.

Tattersall, G. J., D. V. Andrade, and A. S. Abe (2009). Heat exchange from the toucan bill reveals a controllable vascular thermal radiator. Science 325:468–470.

Tieleman, B. I., J. B. Williams, G. Michaeli, and B. Pinshow (1999). The role of the nasal passages in the water economy of crested larks and desert larks. Physiological and Biochemical Zoology 72:219–226.

Todd, W. E. (1924). A new Song Sparrow from Virginia. The Auk 41:147–148.

van de Ven, T. M. F. N., R. O. Martin, T. J. F. Vink, A. E. McKechnie, and S. J. Cunningham (2016). Regulation of heat exchange across the hornbill beak: Functional similarities with toucans? PLOS One 11(5):e0154768. doi: 10.1371/journal.pone.0154768

Van Valkenburgh, B., A. Curtis, J. X. Samuels, D. Bird, B. Fulkerson, J. Meachen-Samuels, and G. J. Slater (2011). Aquatic adaptations in the nose of carnivorans: Evidence from turbinates. Journal of Anatomy 218:298–310.

Vickerton, P., J. Jarvis, and N. Jeffery (2013). Concentration-dependent specimen shrinkage in iodine-enhanced microCT. Journal of Anatomy 223:185–193.

Wolf, B., and G. Walsberg (1996). Respiratory and cutaneous evaporative water loss at high environmental temperatures in a small bird. Journal of Experimental Biology 199: 451–457.

Yokosuka, M., A. Hagiwara, T. R. Saito, M. Aoyama, M. Ichikawa, and S. Sugita (2009a). Morphological and histochemical study of the nasal cavity and fused olfactory bulb of the Brown-eared Bulbul, *Hysipetes amauroti*. Zoological Science 26:713–721.

Yokosuka, M., A. Hagiwara, T. Saito, N. Tsukahara, M. Aoyama, Y. Wakabayashi, S. Sugita, and M. Ichikawa (2009b). Histological properties of the nasal cavity and olfactory bulb of the Japanese Jungle Crow *Corvus macrorhynchos*. Chemical Senses 34:581–593.
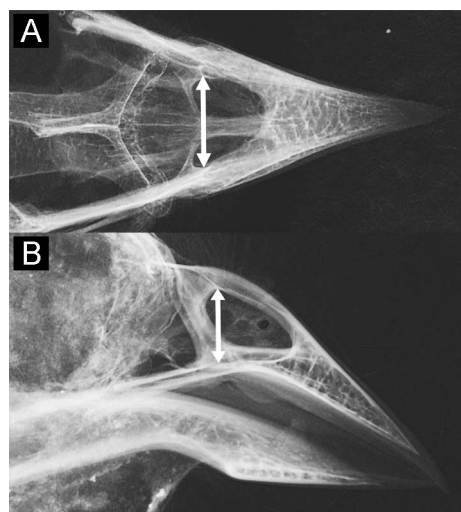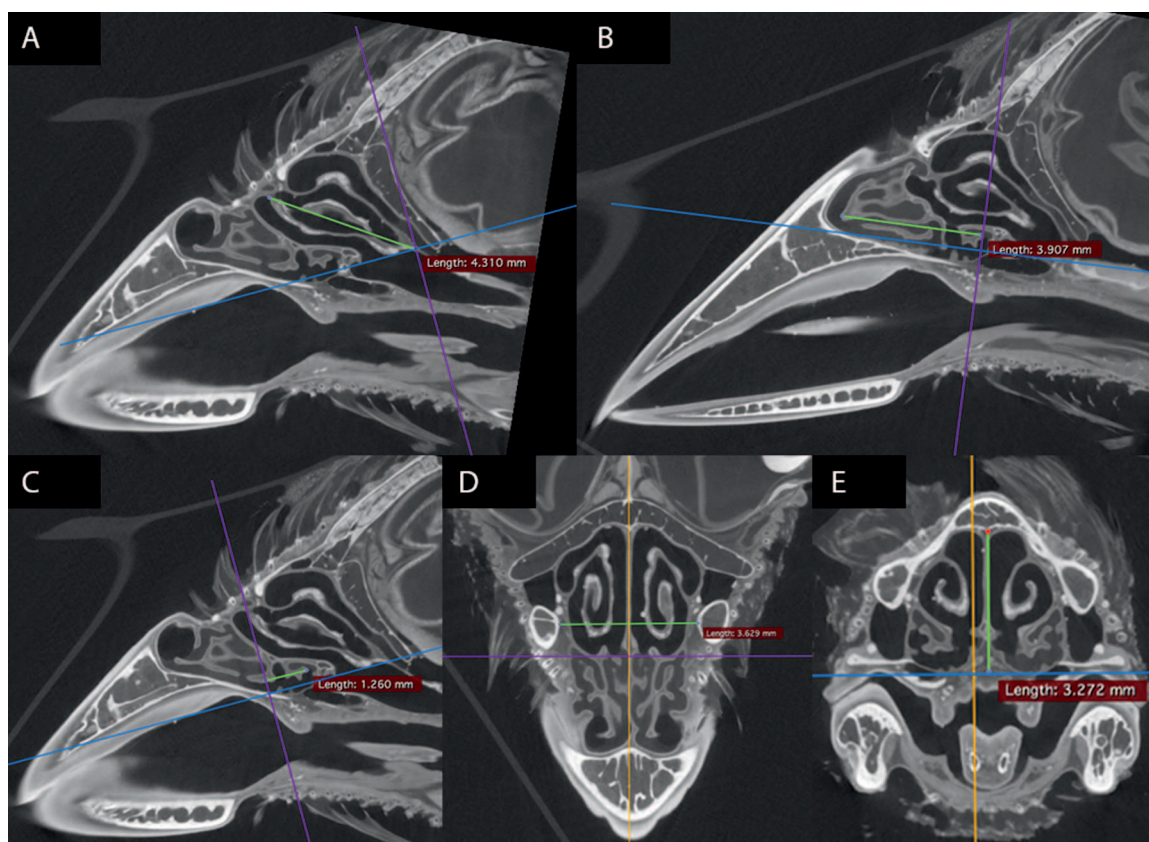
APPENDIX
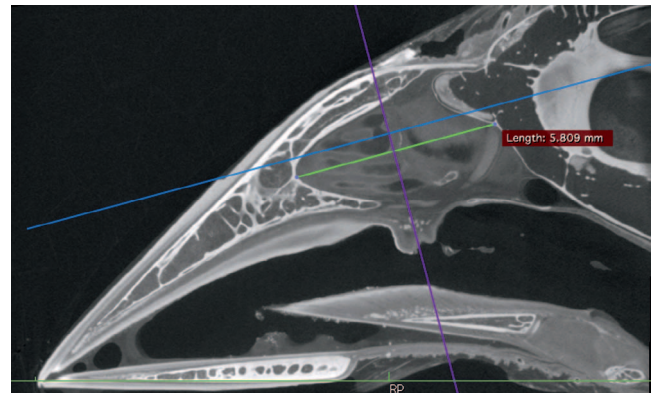
APPENDIX FIGURE 5. Sagittal image of the bill of a Song Sparrow showing the axis along which we extracted cross-sections of the nasal cavity for comparative analyses (green line). The length of the nasal cavity was measured from the sagittal notch in the ectethmoid to the distal end of the bony nasal cavity along the nasal septum, from which we took 10 evenly spaced screenshots parallel to the purple line for analysis. Image derived from CT scans. Blue and purple lines represent the reference axes of the 3D model.
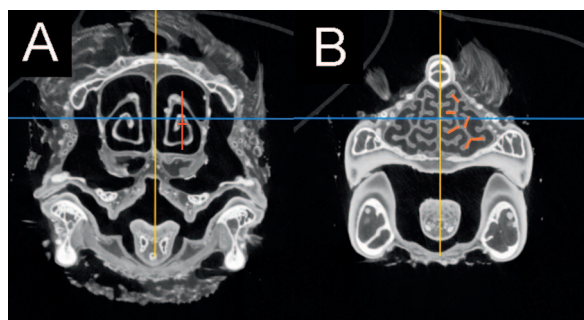
APPENDIX FIGURE 6. Frontal cross-sections used to measure complexity of (**A**) middle conchae (guide shown as red cross) and (**B**) rostral conchae (projections marked in orange; see text for details). Blue and yellow lines are reference axes of the 3D model.

APPENDIX FIGURE 8. (**A**) Dorsal and (**B**) lateral radiographs showing measurements of nasal cavity width and depth, respectively, taken from study skins.

APPENDIX FIGURE 7. Figure of linear measurement locations (green lines) on CT-scan images of a single fluid-preserved specimen. Sagittal sections show: (**A**) middle concha length, (**B**) rostral concha length, and (**C**) concha overlap; a transverse section shows (**D**) nasal cavity width, and a frontal section shows (**E**) nasal cavity depth.